M. Riva, L. Zabeo, E. Joffrin, D. Mazon, D. Moreau, A. Murari, R. Felton,
K. Guenther, X. Litaudon, F. Sartori, C. Taliercio, G. Tresset
and JET EFDA Contributors

Real Time Safety Factor Profile Determination in JET

Real Time Safety Factor Profile Determination in JET

M. Riva[1], L. Zabeo[2], E. Joffrin[2], D. Mazon[2], D. Moreau[2], A. Murari[4], R. Felton[3],
K. Guenther[3], X. Litaudon[2], F. Sartori[3], C. Taliercio[4], G. Tresset[2]
and JET EFDA Contributors*

[1]*Associazione Euratom-ENEA sulla Fusione, C.R. Frascati, 00044 Frascati Italy*
[2]*Association Euratom-CEA, CEA Cadarache, F-13108, St Paul lez Durance, France*
[3]*EURATOM/UKAEA Fusion Association, Culham Science Centre, Abingdon, U.K.*
[4]*Consorzio RFX Associazione ENEA-EURATOM per la Fusione, 4-35127 Padova, Italy*
* *See annex of J. Pamela et al, 'Overview of Recent JET Results and Future Perspectives',
Fusion Energy 2000 (Proc. 18th Int. Conf. Sorrento, 2000), IAEA, Vienna (2001).*

ABSTRACT.

During the last experimental campaigns at JET, one of the main conclusions was that the control of the pressure alone was not sufficient to sustain high performance regimes in steady state and active control of the safety factor profile was also required. In this paper we present the recent implementation at JET of a real-time system to calculate the electron density and the safety factor profiles directly from the line-integrated density and the calibrated Faraday angle measurements. Current density, electron temperature and density profile are now available in real time using magnetic, interfero-polarimeter and electron cyclotron emission data, thus allowing real-time feedback control of these profiles with the heating and current drive actuators available at JET. We present the description of the algorithms, the hardware and software architecture and the first results.

1. REAL TIME Q PROFILE ALGORITHM

In previous experiments, the q-profile control has been performed using a feedback on the internal inductance parameter l_i [1,2]. However, l_i is a global quantity, mainly characterizing the current density in the outer plasma region, and its control is not sufficient to maintain an optimal magnetic shear profile in ITB discharges [3]. Efforts have been made to design a system for determining q-profiles in real time, as a prerequisite for real-time control [4]. The developed algorithm uses, as input signals, the magnetic measurements, the line-integrated densities and Faraday rotation angles obtained from the far-infrared interfero-polarimeter.

To calculate the q profile, the following formula has been used:

$$q = \frac{d\Phi / dV}{d\Psi / dV} \tag{1}$$

Therefore, to calculate q, we need to know the poloidal Ψ and toroidal Φ field profiles. The toroidal field is known, being given by the magnetic measurements in real time, so only the poloidal field profile has to be determined. For this purpose, polarimetric measurements are inverted according to the following integrals

$$N = K\lambda" \int_l n_e(l)dl \tag{2}$$

$$\Delta F = C\lambda^{2"} \int_l n_e(l)B_{||}(l)dl \tag{3}$$

where N is the total accumulated phase, K is a constant ($K = 2.818 \ 10^{-15}$), ΔF is the Faraday rotation angle, n_e is the electron density, $B_{||}$ is the poloidal field component parallel to the laser beam direction of propagation, C is a constant $C = 2.631 \ 10^{-13} \ T^{-1}$), λ is the wavelength mm (195) and the integrals are taken along a line of sight. In total the interferometer-polarimeter at JET sees the plasma along seven chords, four lateral and three vertical chords.

To perform the inversion, a parametric characterization of the magnetic surfaces is required. The Last Closed Magnetic Surface (LCMS) topology is determined on the basis of the external magnetic pick-up coil measurements. To describe the magnetic topology in the plasma interior, the following flux surface parameterization is used [5]:

$$\begin{cases} R = R_{axis} + \Delta(\rho) + \rho cos(\vartheta + \gamma(\rho)sin(\vartheta)) \\ Z = Z_{axis} + \rho K(\rho)sin(\vartheta) \end{cases} \tag{4}$$

where ρ is the radial coordinate, R_{axis} and Z_{axis} the magnetic axis coordinates, $\Delta(\rho)$ the Shafranov shift, $\gamma(\rho)$ the triangularity and $K(\rho)$ is the elongation. $\Delta(\rho)$, $\gamma(\rho)$ and $K(\rho)$ can be determined from the poloidal field and the geometry at the edge.

Once the magnetic surface geometry has been determined, the line-integrated measurements of the interferometer are inverted using a Singular Value Decomposition (SVD) technique, with the following parametrisation for the density:

$$n_e(\rho) = n_0(1 - \rho^2)(1 + p\rho^2 + q\rho^4) + n_w \tag{5}$$

The relations between the three parameters q n n n 0 0 0 p, , and the experimental interferometric measurements can be cast in matrix form [A][N] = [X], where A is the n_{chords} x3 matrix to be pseudo-inverted via SVD and N contains the experimental data. The pedestal value w n is found minimizing, in least-squares sense, the difference between the experimental and calculated values.

Using the same technique the polarimetric measurements can be inverted, starting from the following representation of the poloidal field:

$$B_p^R = -\frac{1}{2\pi R} \frac{\partial \Psi}{\partial \rho} \frac{\partial \rho}{\partial Z} \qquad B_p^Z = \frac{1}{2\pi R} \frac{\partial \Psi}{\partial \rho} \frac{\partial \rho}{\partial R} \tag{6}$$

The flux derivative is parameterized using a polynomial approximation:

$$\frac{\partial \Psi}{\partial \rho} = a_0\rho + a_1\rho^2 + a_2\rho^3 \tag{7}$$

These algorithms can be summarized as in Figure 1.

q-profile validation has been performed on a large database of pulses in different scenarios, showing good agreement with the offline reconstruction code EFIT [4,11]. Fig. 2 shows a comparison between reconstructed profiles.

2. HARDWARE DESCRIPTION

The general real-time system is divided in two sections. The first (Fig.3) is devoted to calculating the Faraday angles and the line-integrated densities, whereas the second (Fig.4) performs the q and n_e profile determination. The first system is based on a VME crate, hosting a VPLS Crate Service Module, three PowerPC CPUs, slow and fast data acquisition boards.

RTDN is the JET real-time data network. RTSS collects and sends signals across JET in real time and the Real Time Central Controller (RTCC) performs the control actions on the JET machine using the heating systems as actuators [8].

The VME system is divided in two real-time subsystems: The Faraday angle (FAR) and the Line-Integrated Density (LID) calculators. The calculation algorithms are the standard ones [4,5]. The real-time Faraday angle system is formed by one powerPC processor and a slow ADC. The system acquires 32 analogue channels at 1 kHz sampling frequency. The 1 kHz hardware interrupt is used as a trigger for this sampling. This operates as a mailbox interrupts to the Power PC. The second hardware signal used is the PRE signal coming from the JET timing and trigger system (CTTS).

The PowerPC processor does all the preprocessing. This is a Motorola MVME5100 VME board with 64 Mbytes of RAM, 400 MHz clock. It is equipped with an ATM PMC PCI board, to allow sending real-time data packets to the Real Time Signal Server (RTSS) without using analogue cables. The Crate Service module is a standard JET CPU board. It accepts a fiber-optic link from CTTS and produces the hardware signals as interrupts.

The slow ADC is a PENTLAND MPV956B analogue I/O board that has 12-bit 320 KHz sampling rate ADC. The channels can be 32 single ended ones or 16 differential ones. The real-time LID system uses two power PC CPUs and a fast ADC. The CPUs are the same as in the FAR system and the ADC is an ICS-130 fast acquisition board, capable of acquiring 32 channels at the maximum speed of 1.2 Msample/sec. In the system the 15 signals (three reference signals and twelve lateral and vertical signals) are acquired at 400 kHz sampling rate. The phase increments of the two sorts of beat signals (100 and 5 kHz) are calculated every 100ms; these are then accumulated to produce one phase value every 0.8 ms, to remain under the 1ms clock tick.

The two CPUs share the work to calculate the line-integrated densities. Every millisecond they send data via a shared memory mechanism to the FAR system that finally sends data to the RTDN.

The second hardware section is shown in Fig.4. It is based on a standard high speed PC equipped with an ATM board to collect all the data coming from the real-time polarimeter, interferometer and ECE diagnostics.

3. SOFTWARE DESCRIPTION

The code development for the VME section was done under vxWorks real-time operating system, which is widely used at JET. The software architecture is described in Fig.5.

The four processes plus two interrupt processes and four semaphores form the software package of the FAR system (the square box in Fig.5). The LID system is more complicated and uses the extended structure illustrated in Fig.3. The description of the FAR system is given first followed by the LID system.

The Start process is the interface with the JET countdown system, and it waits for a queue message. This message contains all the parameters to start a new calculation phase. Then it creates (spawns) the goQ process. The goQ process waits for the JET PRE hardware signal, which means

that a new shot is arriving. Then it spawns the two processes Hist and End and waits for the Dbg semaphore to be taken. When the End process releases the Dbg semaphore, all the data are ready to be stored in the JET post Pulse File data base (JPF) system by the GAP process.

The Hist process is the system core. It acquires 32 channels and calculates the Faraday angles. The output is an ATM packet formed by the polarimetric plus the interferometric data read from the shared memory. The output rate is 10ms. When the shot is finished, it releases the End semaphore. The End process performs the finishing procedures and releases the Dbg semaphore, allowing the system to return to an idle state, waiting for the next shot.

The same software structure holds for the real-time LID system but in this case there is a complication, because the acquisition speed is very high (400KHz) and the output has to be released every millisecond. So we used the Front Panel Data Port (FPDP) option in the ICS-130. In such a modality, we store 320 samples for each acquired channel, performing the LID calculations in less than 1ms.

To achieve the necessary throughput, we have split the calculation between two CPUs, so each of these writes its results in the shared memory in the required time without loss of data. The software architecture change is the addition of two supplementary processes that detach the "fast" real-time side (400KHz) from the "slow" one (1kHz). The goQ process spawns the kg1 process, which, in turn, spawns the kg1_sim. The "fast" and "slow" sides are synchronized using a supplementary semaphore called "read". We have added another feature to the system allowing the JET central acquisition system to "poll" the internal status. The system responds telling the actual state.

4. PROFILE CONTROL AND EXPERIMENTAL RESULTS

The control experiments in the previous campaigns, using simple control schemes based on scalar measurements like ρ_{T*MAX}, have shown limitations due to the strong non-linear coupling between the pressure and current-density profiles. Model-based control techniques have been applied to design a multiple-input multiple-output (MIMO) controller, to achieve steady state regimes in JET with a given q-profile [9]. A new approach has been pursued [10], taking into account the spatial structure of the system and considering the interaction between various measured quantities at different radii through an infinite-dimensional operator. To overcome the difficulties of the non-linearities in the design of the controllers, linear system around a target equilibrium has been chosen. This infinite-dimensional system is approximated using a truncated SVD technique, thus becoming a linearised Laplace transform model of the form $Q(s) = K(s) P(s)$ where Q represents the safety factor vector (or a combination of safety factors and ρ_{T*}), K the approximation of the infinite-dimensional operator and P the input powers.

As a typical application of the control scheme, we tried to reach a predefined q-profile target, keeping all other plasma parameters constant. The feedback control was performed on five points of the q-profile located at fixed normalized radii (r/a = 0.2, 0.4, 0.5, 0.6, 0.8). The global result is reported in Fig. 6, where the combined control action on all the profiles is shown [12]. In this pulse, Lower Hybrid additional power was used as actuator.

CONCLUSION AND FUTURE WORKS.

Real-time Faraday rotation angles and line-integrated densities are now available at JET, with a time resolution of up to 1ms. This real-time data allows the calculation of the current-density profile every 50ms, sufficient for the JET real-time requirements. Using this tool, the first successful demonstration of a feedback control of the safety factor profile during a low-density phase has been accomplished using LH as the only actuator. In the next campaigns, a combined control using heating and current drive systems will be applied to both pressure and current profiles aiming at extending the duration of ITB plasmas. Moreover, since the interferometer can be affected by fringe jumps in H-mode regimes, a dedicated algorithm is under development to correct them in real time [7].

REFERENCES

[1]. E. Joffrin, P. Defrasne, Rev. of Scient. Instrum, **73**, 2266 (2002)

[2]. O. Barana et al 2002, Plasma Phys. Control Fusion., submitted for publication

[3]. M. Riva et al, Proc 19th IEEE/NPSS Symp. On Fusion Eng. (SOFE) (Atlantic City, USA Jan 2002)

[4]. L. Zabeo et al, 2002, Plasma Phys. Control Fusion, submitted for publication

[5]. J.P. Christiansen, Journal of computational Physics 73, 85-106 (1987)

[6]. S.E. Segre, Plasma Phys. **20**, (1978) 295

[7]. P. Innocente et al, Rev. of Scient. Instrum., submitted for publication

[8]. R. Felton et al, Real Time Plasma Control at JET using an ATM Network, JET-P(99)27.

[9]. D. Moreau, I. Voitsekhovitch, Nuclear Fusion **39**, 685 (1999)

[10]. D. Moreau et al, Proc. Of the 3 rd IAEA TCM, May 2002, to be published in Nucl. Fusion

[11]. L.L. Lao et al, Nuclear Fusion **30** (6), (1990) 1035

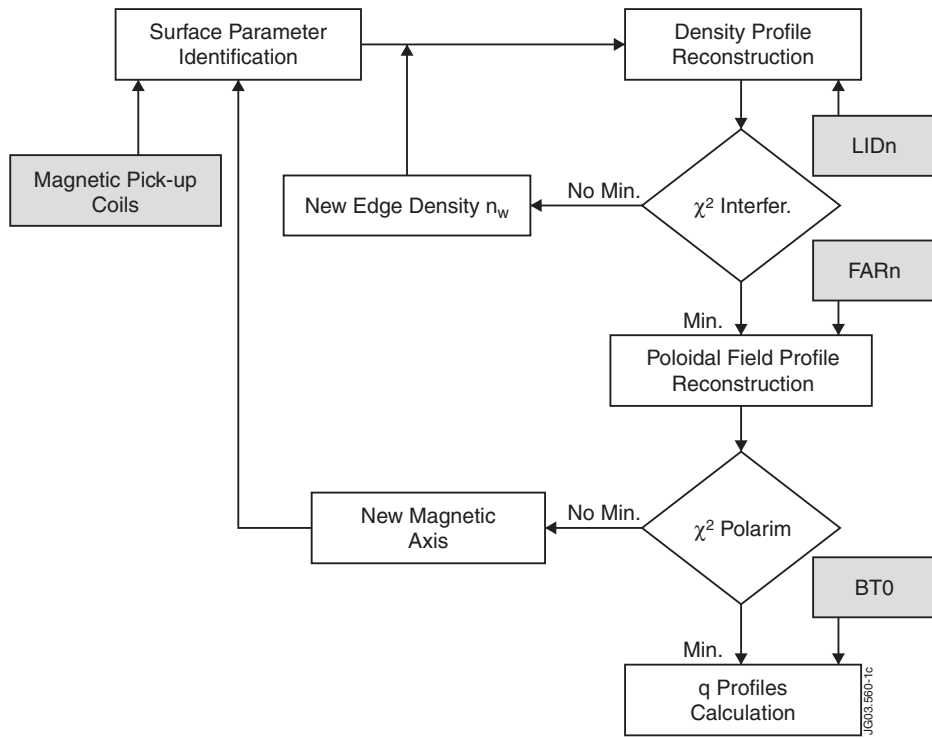[12]. D. Mazon et al, 2002 in Controlled Fusion and Plasma Physics (proc. 29th Eur. Conf. Montreaux)

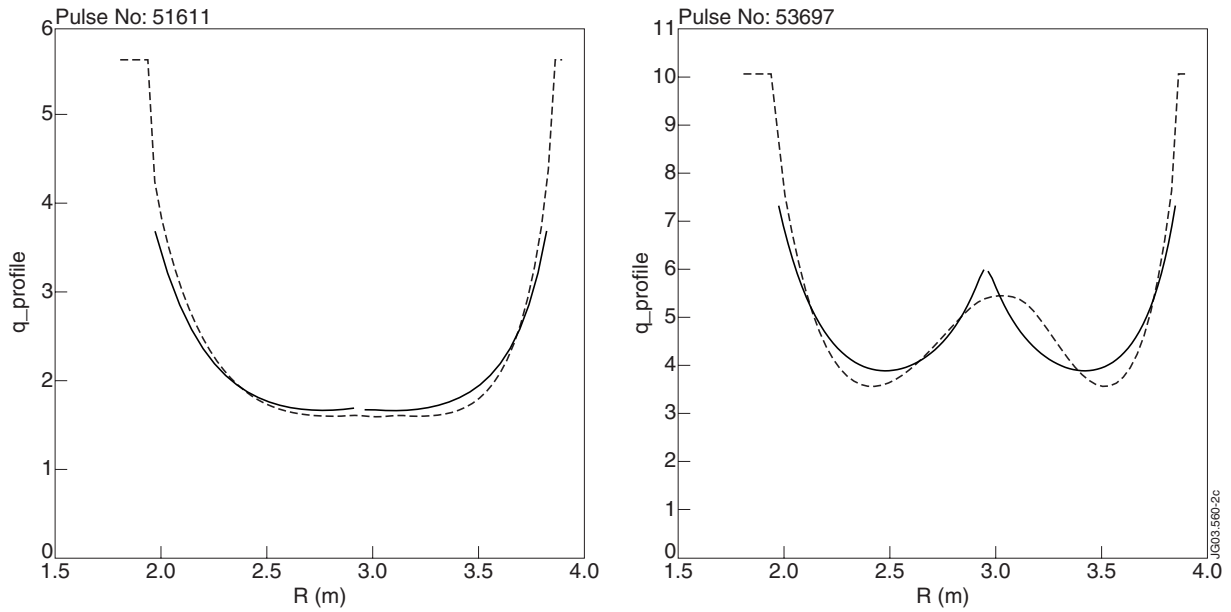*Figure 1: Block diagram of q-profile calculation.*

Figure 2: q-profile reconstruction results (solid line) vs offline code (dashed line) in two different scenarios.
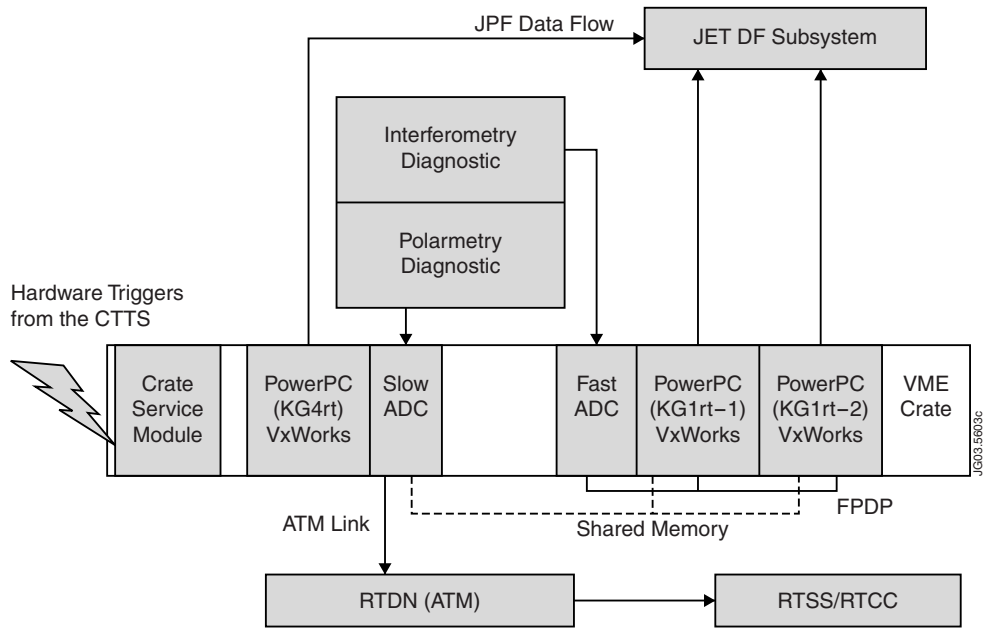
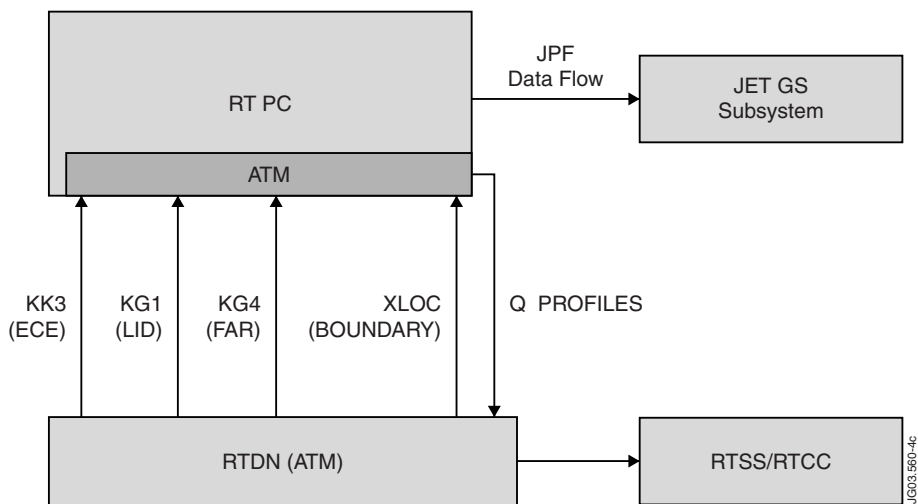*Figure 3: Hardware block diagram of FAR and LID systems.*

*Figure 4: Block diagram of the q-profile hardware. The system
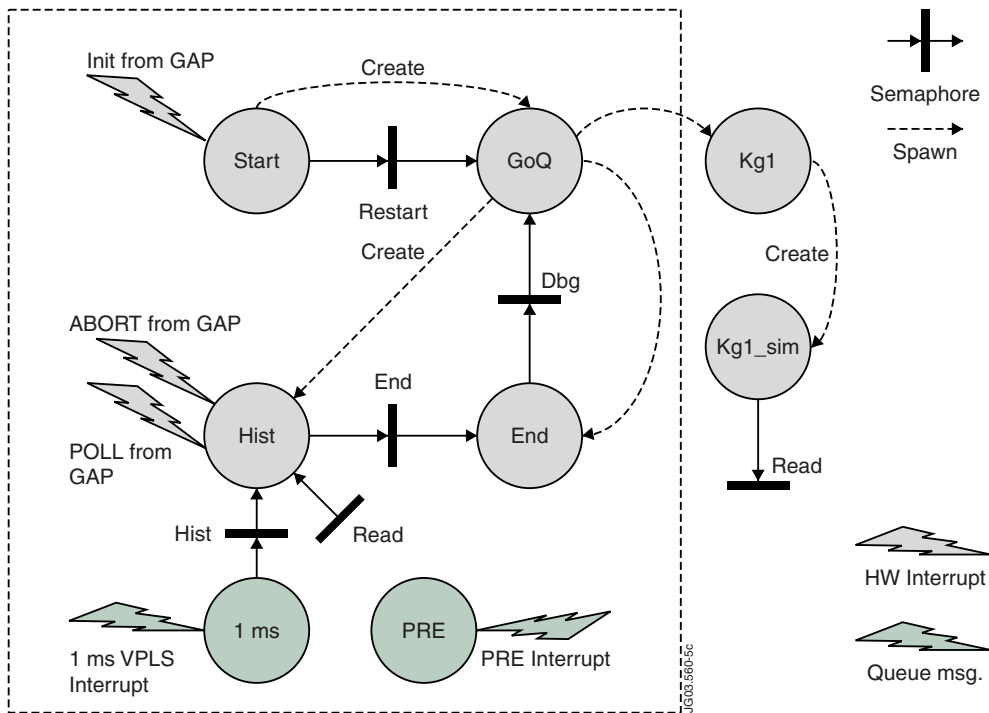receives all its data via ATM, producing the output in the same way.*

Figure 5: Block diagram of the software processes involved in the Line Integrated Densities and Faraday angles calculation.
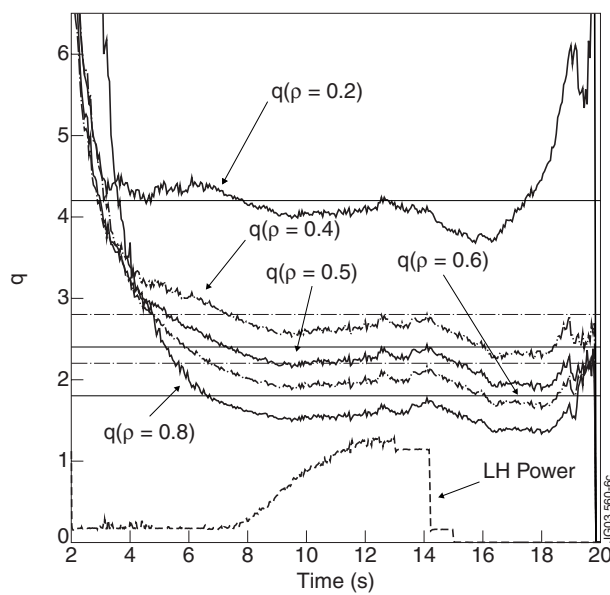

Figure 6: Pulse No: 55873. q profile time evolution for five different radii compared with the references.